Risk assessment of mega-city infrastructures related to land subsidence using improved trapezoidal FAHP

Hai-Min Lyu [a], Shui-Long Shen [a,b,*], Annan Zhou [c], Jun Yang [d]

[a] Department of Civil and Environmental Engineering, College of Engineering, Shantou University, Shantou, Guangdong 515063, China
[b] Key Laboratory of Intelligent Manufacturing Technology (Shantou University), Ministry of Education, Shantou, Guangdong 515063, China
[c] Discipline of Civil and Infrastructure, School of Engineering, Royal Melbourne Institute of Technology (RMIT), Victoria 3001, Australia
[d] Department of Civil Engineering, The University of Hong Kong, Pokfulam, Hong Kong Special Administrative Region

HIGHLIGHTS

- Developed a method to assess risk of infrastructures using trapezoidal FAHP
- Proposed a new questionnaire to determine trapezoidal fuzzy numbers in trapezoidal FAHP
- Land-subsidence-induced risk in Shanghai is assessed using trapezoidal FAHP and AHP
- The results were validated by the current prevention zone of land subsidence in Shanghai.

GRAPHICAL ABSTRACT
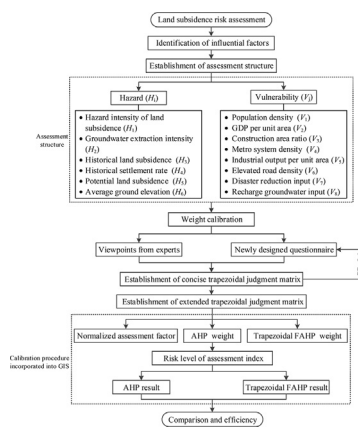
ARTICLE INFO

ABSTRACT

This study presents an improved trapezoidal fuzzy analytic hierarchy process (FAHP) to assess the risk of mega-city infrastructures related to land subsidence. The trapezoidal fuzzy numbers are used to express the relative importance between assessment factors. A new questionnaire is proposed in this study to collect judgements from consulting experts. Both the original AHP and the trapezoidal FAHP with the new questionnaire are applied to assess the risk of infrastructures in relation to land subsidence in Shanghai. The risks assessed using the trapezoidal FAHP at locations with significant infrastructures are higher than those assessed using the original AHP. This indicates that the trapezoidal FAHP method with the new questionnaire can be used to effectively capture the high risks for significant industrial infrastructures related to land subsidence. Moreover, the obtained results were compared with the current land subsidence prevention zone, and it was observed that the existing land subsidence prevention zone in government management guidelines does not sufficiently consider the vulnerability of significant infrastructures.

* Corresponding author at: Department of Civil and Environmental Engineering, College of Engineering, Shantou University, Shantou, Guangdong 515063, China.
E-mail addresses: lvhaimin12@163.com (H.-M. Lyu), shensl@stu.edu.cn (S.-L. Shen), annan.zhou@rmit.edu.au (A. Zhou), junyang@hku.hk (J. Yang).

1. Introduction

Land subsidence is a geological disaster induced by natural factors such as consolidation of newly reclaimed ground, peat carbon-

ation, and earthquakes. It can also be caused by anthropic activities including the exploration of underground resources (Yi et al., 2010; Shen and Xu, 2011; Shen et al., 2013; Xu et al., 2019; Wang et al., 2019), underground construction (Godschalk, 2003; Shen et al., 2017; Wu et al., 2017a), long-term operation of urban facilities (Shen et al., 2014), and the creep of soils (Yin et al., 2011, 2014, 2017, 2018; Zhu et al., 2016). Underground construction causes changes in geo-environmental conditions through the recharge and discharge of groundwater (Lee and Park, 2013; Shen et al., 2017; Wu et al., 2019). Infrastructure in a mega-city may be damaged if land subsidence occurs. Numerous artificial groundwater recharge projects have been conducted to solve land subsidence problems in Shanghai. For example, Shen et al. (2017) conducted research on the use of pumping and artificial groundwater recharging in a shallow aquifer for controlling land subsidence.

In Shanghai (the largest city in China), land subsidence has been measured and recorded since 1921. Land subsidence was generally induced by the pumping of groundwater from aquifers (Shen and Xu, 2011). From 1921 to 1949, land subsidence in Shanghai increased gradually; however, from 1950 to 1965, the subsidence accelerated (Chai et al., 2004; Xu et al., 2016; Wu et al., 2016, 2017a). Since 1966, artificial recharging in shallow aquifers has been conducted, and the subsidence was maintained at a small value until 1989. After 1990, the subsidence rate increased again owing to the effect of underground structures obstructing the aquifers (Xu et al., 2012 Ma et al., 2014). It has been acknowledged that land subsidence is a threat to underground infrastructures such as the deep foundations of high-rise buildings and metro tunnels in Shanghai (Shen et al., 2014). Land subsidence causes the severe settlement of metro lines and buildings in Shanghai (Wu et al., 2017b), and the maximum settlement of line No. 1 is approximately 2 m; therefore, realising the control of land subsidence is an urgent task.

2. Literature review

With respect to the influence of land subsidence on infrastructure, both the quantitative prediction and risk assessment of infrastructure play a significant role in decision-making. Land subsidence can be predicted using either a mathematical or numerical model. The mathematical model employs the statistical method to characterise the former subsidence events for predicting future behaviour (Xu et al., 2012; Ma et al., 2014). The numerical model comprises the use of the finite element method or finite difference method to predict both groundwater seepage and ground deformation (Shen et al., 2013; Shen and Xu, 2011; Wu et al., 2017b). However, the method used to assess the damage of infrastructures in relation to land subsidence is still unclear. For example, Wu et al. (2017b) recently proposed the use of a simple approach to identify the contribution of land subsidence to metro tunnel settlement in the soft deposits of Shanghai. The method proposed by Wu et al. (2017b) is a mathematical model based on the measured data of both land subsidence and tunnel settlement. However, (Wu et al.'s (2017b) method comprises an evaluation of only the behaviour of one metro line under the land subsidence environment and cannot be used to evaluate the overall risk of the infrastructure system within the land subsidence environment.

The risk related to land subsidence can be evaluated using various mathematical methods, such as the analytic hierarchy process (AHP) (Saaty, 1996, Saaty, 2004), Bayesian network rules (Jin et al., 2016, 2018), fuzzy mathematics method (Sierra et al., 2018; Jin et al., 2019a, Jin et al., 2019b), and Gray method (Ishikawa et al., 1993). The existing assessment methods for risk related to land subsidence primarily comprise the use of the traditional AHP method (Kamal et al., 2013). In the original AHP, a single weight index is used to evaluate the relative importance between assessment factors. The relative importance between two factors is determined according to the judgements from experts. However, in the majority of cases, the judgements from several experts vary, which may result in a bias in the result evaluated using a single weight index. To overcome these deficiencies, the use of fuzzy AHP (FAHP) has been proposed to improve the application of the original AHP (Laarhoven and Pedrycz, 1983; Lyu et al., 2018, 2019a, 2019b, 2019c; Sadiq and Tesfamariam, 2009; Zou et al., 2013).

The FAHP includes the interval FAHP, triangular FAHP, and trapezoidal FAHP approaches. Instead of the use of a crisp number as in the original AHP, the interval, triangular, and trapezoidal FAHP methods adopt the interval, triangular, and trapezoidal fuzzy numbers, respectively, to express the relative importance of the assessment factors (Zou et al., 2013; Prascevic and Prascevic, 2017). The use of a fuzzy number can decrease the resulting deficiencies as compared to those obtained while using a crisp number (Lyu et al., 2019a-d). For example, an interval fuzzy number has lower and upper bound values; a triangular fuzzy number has lower, medium, and upper bounds; and a trapezoidal fuzzy number has lower, left-medium, right-medium, and upper bounds. The determination of a fuzzy number involves the determination of several bound values, which is therefore difficult to realise while using the traditional questionnaire. Zou et al. (2013) employed the ordinary trapezoidal FAHP to assess flood risk by using the traditional questionnaire. However, it should be noted that this research (Zou et al., 2013) did not present the process for determining the trapezoidal fuzzy number, which is a key but difficult point in the application of the FAHP. Generally, consulting an expert is a useful method that can be used to determine the importance degree of assessment factors. The traditional questionnaire comprises the use of a pairwise comparison in a consulting process (Li et al., 2013). The pairwise comparison has the following two distinct shortcomings: (i) the assessment model, which comprises large influential factors, is complex; and (ii) an inconsistency may exist in the judgment matrix obtained from the pairwise comparison. To overcome the limitations of traditional questionnaires, a new questionnaire is presented to easily collect the importance degree of the assessment factors obtained from the experts consulted. The proposed questionnaire is used to determine the trapezoidal fuzzy number using a trial calculation. The trapezoidal FAHP with the new questionnaire is used for assessing the infrastructure risk related to land subsidence.

The assessment of the infrastructure risk related to land subsidence is challenging, because there are many uncertainties when considering the interaction between land subsidence and infrastructure. Accordingly, a multi-index system should be employed in the risk assessment. The objective of this study is to develop a method to assess the risk of mega-city infrastructures related to the land subsidence based on the trapezoidal FAHP method. To obtain reliable results, a new questionnaire is proposed for determining the fuzzy number in the FAHP. The proposed approach is used to assess the land-subsidence-induced risk of infrastructures in Shanghai.

3. Methodology

3.1. Risk assessment model

The mechanism of the infrastructure risks related to land subsidence is associated with hazard-inducing factors and a hazard-breeding environment as the terms of vulnerability of a disaster-bearing body. Therefore, the risks related to land subsidence are a combination function of the hazard index and vulnerability index (Wang et al., 2014), which can be described using Eq. (1).

$$Risk = Hazard \otimes Vulnerability \tag{1}$$

where $\otimes$ represents the overlay analysis in geographic information system (GIS). This equation is used to express the definition of risk.

Generally, the indices of hazard and vulnerability comprise several factors. Each factor has a different weight for the risk assessment. Therefore, the assessment model can be specified using Eq. (2).

$$Risk = \sum_{i=1}^{n} h_i H_i \otimes \sum_{k=1}^{n} v_k V_k \tag{2}$$

where H_i and V_k are the normalised factors of hazard and vulnerability, respectively, which can be obtained using Eqs. (3) and (4), respectively; h_i, and v_k are the weight coefficients of the aforementioned factors, respectively.

Positive factor:

$$x_{ij} = \frac{x_{ij0} - x_{min}}{x_{max} - x_{min}} \tag{3}$$

Negative factor:

$$x_{ij} = \frac{x_{max} - x_{ij0}}{x_{max} - x_{min}} \tag{4}$$

where x_{ij} is the normalised value of the assessment factor; x_{ij0} is the original value; and x_{max} and x_{min} are the maximum and minimum values, respectively. If the risk level decreases as the assessment factor value increases, this factor is a negative factor; otherwise, the factor is a positive. Subsequent to the normalisation, the assessment factors range from 0 to 1.

3.2. New questionnaire

To reflect the real situation during decision-making, a new questionnaire is designed for obtaining the viewpoints of experts. Table 1 presents a comparison between the traditional and new questionnaires. Compared with the traditional questionnaire, the new questionnaire can handle the assessment structure, which comprises a large number of factors, by assigning scores to the assessment factors. Moreover, a consistent judgment from the new questionnaire can be guaranteed by using a trial calculation, whereas an inconsistency may exist in the judgment obtained using the traditional questionnaire. The proposed questionnaire is presented in the companion data article (Lyu et al., 2019e). Instead of asking experts to compare any two factors with five choices, the proposed questionnaire can capture the subtle changes in expert judgements regarding how strongly a factor poses challenges on the risks in terms of nine scores via a table. The nine scores express the influence level of a factor on the risk, from 1 as equally important to 9 as extremely important. The factor with a greater score has a higher priority. This is an effective method to collect various viewpoints from a large number of experts for solving a complex problem. In the consulting process, each factor was

considered and given a score ranging from 1 to 9 to reflect its influence level on the risks. Each of the nine scores could be assigned to a maximum of two factors. This restriction can guarantee that all nine scores are assigned, thus ensuring a consistent judgement matrix. According to all the expert viewpoints, analysts can perform pairwise comparisons to establish the judgement matrix by satisfying the consistency requirement. Based on the obtained experts' opinions, the trapezoidal fuzzy number can also be determined. The details of the application of the proposed method are discussed in the following context.

3.3. Trapezoidal FAHP
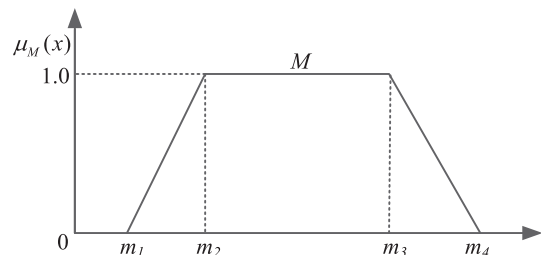
3.3.1. Trapezoidal fuzzy number

The trapezoidal fuzzy number is denoted as $M = (m_1, m_2, m_3, m_4)$. Fig. 1 shows the membership function of a trapezoidal fuzzy number. The parameters m_1 and m_4 are the lower and upper limits of M, respectively; m_2 and m_3 are the interval variables of M (Zou et al., 2013). The membership function of $\mu_M(x)$ for M is defined as presented in Eq. (5). As shown in Fig. 2, if $m_2 = m_3$, M becomes a triangular fuzzy number; if $m_1 = m_2$ and $m_3 = m_4$, M becomes an interval number; if $m_1 = m_2 = m_3 = m_4$, M becomes a crisp value. Therefore, a trapezoidal fuzzy number can arithmetically handle and intuitively interpret fuzzy numbers in a variable manner. Hence, the authors selected the trapezoidal FAHP for assessing the risk induced by land subsidence on infrastructures. Trapezoidal FAHP comprises the use of trapezoidal fuzzy numbers, which is used to express the relative importance of assessment factors. However, it is difficult to determine the trapezoidal fuzzy numbers in the application of the trapezoidal FAHP.

$$\mu_M(x) = \begin{cases} 0, & (x < m_1) \\ \frac{x - m_1}{m_2 - m_1}, & (m_1 \leqslant x \leqslant m_2) \\ 1, & (m_2 \leqslant x \leqslant m_3) \\ \frac{m_4 - x}{m_5 - m_4}, & (m_3 \leqslant x \leqslant m_4) \\ 0, & (x > m_4) \end{cases} \tag{5}$$

The new questionnaire proposed in this study was used to determine the trapezoidal fuzzy numbers and establish a consistent judgement matrix in the trapezoidal FAHP. According to the statistics obtained from the new questionnaire, each influencing factor is given as an interval value with different selection times. Therefore, the pairwise comparison between two influencing factors can be described as a ratio using the statistical values. This ratio can be approximated using a concise trapezoidal fuzzy number. Finally, the trapezoidal fuzzy number can be determined to express the relative importance between the influencing factors.

3.3.2. Weight calibration

According to the definition of the trapezoidal fuzzy judgement matrix, if $C = [M_{ij}]_{n \times n}$ is a trapezoidal fuzzy judgement matrix,

Table 1
Comparison between the traditional and new questionnaires.

Type	Traditional questionnaire	New questionnaire
Basic theory	Pairwise comparison	Pairwise comparison
Consulting process	Pairwise comparison	Assign score to each factor
Large number of factors	Complex	Simple
Consistency of judgment	Inconsistency may exist	Consistency can be guaranteed by trial calculation

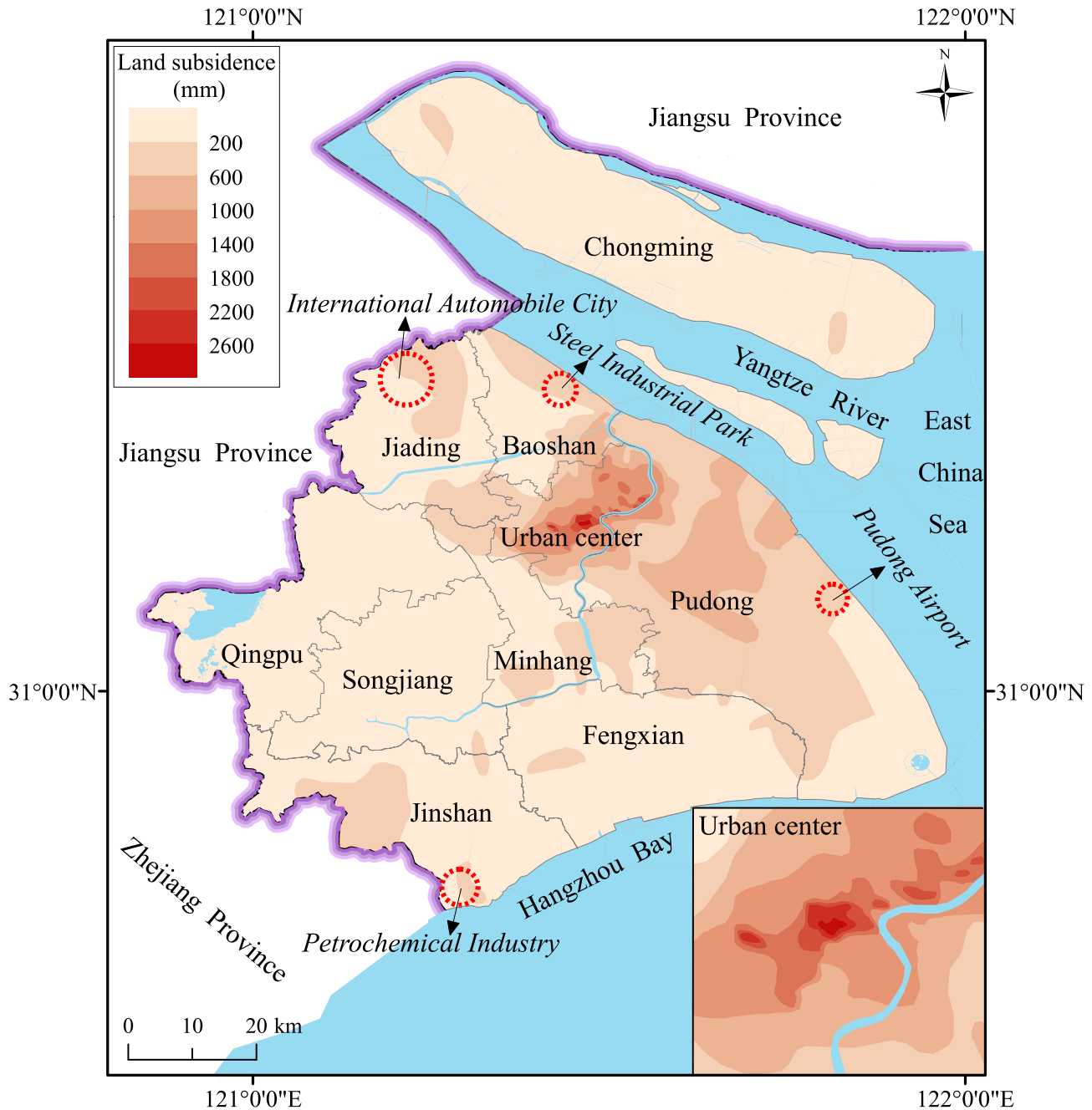**Fig. 1.** Membership function of a trapezoidal fuzzy number.

Fig. 2. Overall land subsidence in Shanghai (from 1921 to 2010).

where $M_{ij} = (m_{1ij}, m_{2ij}, m_{3ij}, m_{4ij})$ is a trapezoidal fuzzy number, and a real value $m_{2ij} < p_{ij} < m_{3ij}$ exists that can satisfy the consistency of the concise matrix $P = [P_{ij}]_{n \times n}$, subsequently the trapezoidal fuzzy judgement matrix $C = [M_{ij}]_{n \times n}$ satisfies the consistency demand. Based on this definition, when the judgement matrix consisting of the concise fuzzy number satisfies the consistent requirement, each element in the judgement matrix can be replaced by a trapezoidal fuzzy number. Finally, the consistent judgement matrix consisting of trapezoidal fuzzy numbers can be determined. Thus, the trapezoidal fuzzy weight can be calibrated using the following steps:

Step 1: Based on the connection of the viewpoints from experts, the analysts can establish the concise trapezoidal judgement matrix $P = [P_{ij}]_{n \times n}$ with an ordinary assignment value in the AHP. The linguistic variables and corresponding trapezoidal fuzzy

number as well as the ordinary number are listed in the data article (Lyu et al., 2019e).

Step 2: The consistency of the concise trapezoidal judgement matrix $P = [P_{ij}]_{n \times n}$ is tested. The value of the consistency ratio (CR) is then used for testing the consistency of the matrix $P = [P_{ij}]_{n \times n}$. This can be calculated using Eq. (6).

$$CR = \frac{CI}{RI} \tag{6}$$

where $CI = (\lambda_{max} - n)/(n-1)$, and λ_{max} is the largest eigenvalue of the judgement matrix, which can be calculated based on Eq. (7). RI is the average random consistency index (Zou et al., 2013). We have $CR \leq 0.05$ when $n = 3$; $CR \leq 0.08$ when $n = 4$, and $CR < 0.1$ when $n \geq 5$. Thus, the concise judgement matrix satisfies the consistency demand.

$$\lambda_{\max} = \sum_{i=1}^{n} \frac{\sum_{j=1}^{n} a_{ij} w_i}{n w_i} \qquad (7)$$

Step 3: An extended trapezoidal judgement matrix with TFNs is established. According to the concise trapezoidal judgement matrix and the linguistic variables with the corresponding trapezoidal fuzzy number listed in the data article (Lyu et al., 2019e), the extended trapezoidal fuzzy judgement matrix $C = [M_{ij}]_{n \times n}$ can be established.

Step 4: The fuzzy weight of the trapezoidal fuzzy judgement matrix $C = [M_{ij}]_{n \times n}$ is calculated. The fuzzy weight is calculated using the geometric average method as shown in Eq. (8).

$$\overrightarrow{w}_j = (w_{j1}, w_{j2}, w_{j3}, w_{j4}) = \left(\frac{m_{1i}}{m_4}, \frac{m_{2i}}{m_3}, \frac{m_{3i}}{m_2}, \frac{m_{4i}}{m_1} \right) \qquad (8)$$

where w_{j1}, w_{j2}, w_{j3}, and w_{j4} are the fuzzy weights of the trapezoidal fuzzy judgement matrix, and $0 < w_{j1} < w_{j2} < w_{j3} < w_{j4} < 1$, whereas m_{1i}, m_{2i}, m_{3i}, and m_{4i} are the values of the trapezoidal fuzzy judgement matrix $C = [M_{ij}]_{n \times n}$, and they can be calculated using Eq. (9).

$$m_{1i} = \left(\prod_{j=1}^{n} m_{2ij} \right)^{1/n}, \quad m_{2i} = \left(\prod_{j=1}^{n} m_{2ij} \right)^{1/n}, \quad m_{3i} = \left(\prod_{j=1}^{n} m_{3ij} \right)^{1/n}, \quad m_{4i} = \left(\prod_{j=1}^{n} m_{4ij} \right)^{1/n}$$
$$m_1 = \sum_{j=1}^{n} m_{1j}, \quad m_2 = \sum_{j=1}^{n} m_{2j}, \quad m_3 = \sum_{j=1}^{n} m_{3j}, \quad m_4 = \sum_{j=1}^{n} m_{4j} \qquad (9)$$

4. Assessment of land subsidence risk in Shanghai

4.1. Background

Shanghai is located in the east of China, which is surrounded by the Jiangsu Province in the north, Zhejiang Province and Hangzhou Bay in the south, and the East China Sea in the east. The average elevation of Shanghai is between 3 and 5 m above sea level (Shen and Xu, 2011; Xu et al., 2012, 2016). The geological formation of Shanghai mainly comprises soft soil. The groundwater table is approximately 2 m below the ground surface. According to the Shanghai Geotechnical Investigation Code (DGJ08-37-2012), the soil type at a depth of 2 m is mixed soil with sand (5%), silt (55%), and clay (40%). Fig. 3 shows the administrative region and overall distribution of land subsidence in Shanghai from 1921 to 2010. As shown in Fig. 3, the greatest land subsidence in the urban area is approximately 2.6 m. Land subsidence causes many problems in urban infrastructures, and therefore, countermeasures should be adopted to prevent the damage induced by land subsidence. Hence, the risk assessment for infrastructures induced by land subsidence should be evaluated, and the infrastructure risk zoning map thus obtained could be helpful to the government and other relevant authorities.

Shanghai has a population of over 25 million on a land area of 6530 km², which is divided into 10 districts, including the Urban Centre, Baoshan, Jiading, Pudong New Development District (hereafter called Pudong district), Fengxian, Jinshan, Minhang, Songjinag, Qingpu, and Chongming. The gross domestic product (GDP) of Shanghai is 28,178 billion RMB (4495.46 billion dollars) (SSY, 2017). Each district has a different GDP output. Large-scale municipal facilities also exist, such as the metro system, Pudong and Hongqiao International Airports, viaducts, underground roads, large-scale bridges, tunnels passing through the Huangpu River,

and high-speed railway stations. Furthermore, large-scale industrial facilities exist, e.g. the steel industrial park in Baoshan, automobile city in Jiading, and petrochemical industry in Jinshan and Pudong (see Fig. 2). Land subsidence threatens the safety of these municipal and industrial facilities. To protect these facilities, the Shanghai Municipal Government invests a large amount of funds.

4.2. Assessment process

Fig. 3 shows the flow chart of the procedure for assessing the infrastructure risk induced by land subsidence. The assessment procedure includes two major sections, including (1) the assessment structure and (2) the calibration process in GIS. The procedure can be described in detail as follows: (1) the influential factors are identified and the assessment structure is established; (2) the experts' judgements are collected using the new questionnaire; (3) the concise judgement matrix is established using a single number according to the viewpoints of the experts; (4) the single number used to establish the extended judgement matrix is replaced using the trapezoidal fuzzy number; (5) the AHP weight and trapezoidal fuzzy weight of the assessment factors are calculated; (6) the risk level of the assessment index is obtained using the normalised assessment factors with their corresponding weights. Using the aforementioned procedure, the assessment results based on the AHP and the trapezoidal FAHP can be obtained. To demonstrate the efficiency of the trapezoidal FAHP with the new questionnaire, the assessed results were compared with the current planning zone for land subsidence in Shanghai.

4.2.1. Identification of influential factors

The influential factors to hazard and vulnerability can be identified from previous studies on land subsidence (Xu et al., 2012, 2013; Ma et al., 2014), including the causes of subsidence, record of subsidence, population distribution, urban construction, and GDP distribution. Based on field investigations, mechanical analyses, and the accessibility of a factor (Shen and Xu, 2011; Shen et al., 2013; Ma et al., 2014), the following six hazard-related factors are identified in this analysis: the hazard intensity of land subsidence (H_1), groundwater extraction intensity (H_2), historical land subsidence (H_3), historical subsidence rate (H_4), potential land subsidence (H_5), and average ground elevation (H_6). Based on their contributions to land subsidence, these factors are ranked from H_1 to H_6. According to their significance to life and property, the vulnerable factors of the infrastructures include the following: population density (V_1), GDP per unit area (V_2), construction area ratio (V_3), metro system density (V_4), industrial output per unit area (V_5), elevated road density (V_6), disaster reduction input (V_7), and recharge groundwater input (V_8). Moreover, urban development has resulted in many underground structures (e.g. pile foundations of high-rise buildings, metro systems, and underground transportation tunnels) in aquifers I and II in Shanghai (Xu et al., 2012; Qiao et al., 2017; Peng and Peng, 2018). These underground structures block the seep-
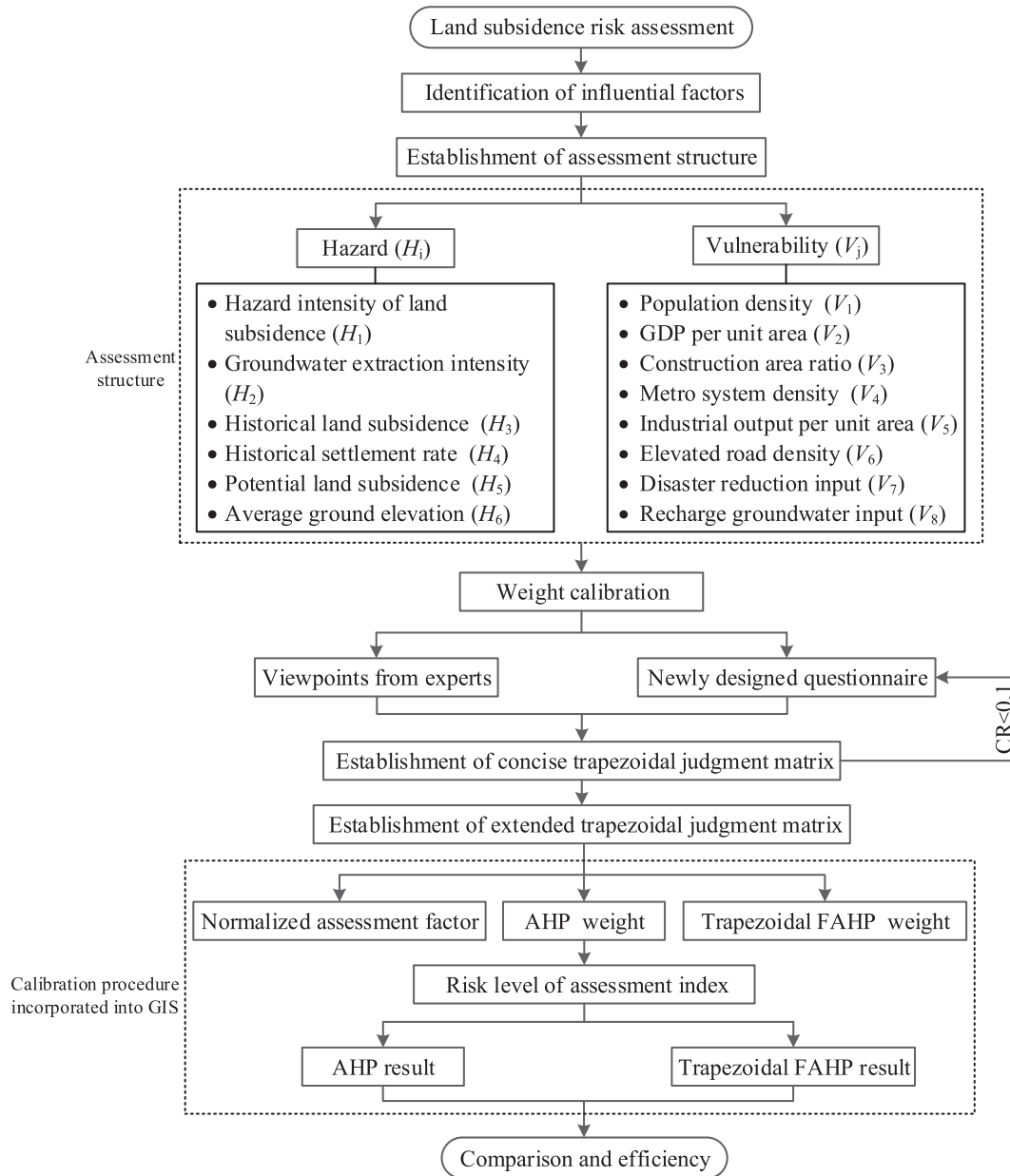
Fig. 3. Flowchart of the assessment procedure for the risk induced by land subsidence.

Table 2
Weights of assessment factors from trapezoidal FAHP and AHP methods.

Assessment index			Assessment factors		
Index	AHP (w)	Trapezoidal FAHP $(\vec{w}_j)$	Factor	AHP (w)	Trapezoidal FAHP $(\vec{w}_j)$
H_i	0.45	(0.25, 0.3333, 0.5385, 0.6667)	H_1	0.2415	(0.1985, 0.2040, 0.2087, 0.2185)
			H_2	0.2279	(0.1803, 0.1812, 0.1901, 0.1985)
			H_3	0.1718	(0.1613, 0.1625, 0.1722, 0.1788)
			H_4	0.1539	(0.1531, 0.1551, 0.1571, 0.1620)
			H_5	0.1223	(0.1516, 0.1528, 0.1560, 0.1593)
			H_6	0.0908	(0.1117, 0.1179, 0.1300, 0.1387)
V_k	0.55	(0.3157, 0.4118, 0.6495, 0.8)	V_1	0.2684	(0.1878, 0.1887, 0.1920, 0.1977)
			V_2	0.2170	(0.1663, 0.1674, 0.1738, 0.1794)
			V_3	0.1665	(0.1393, 0.1418, 0.1479, 0.1520)
			V_4	0.1265	(0.1319, 0.1330, 0.1350, 0.1358)
			V_5	0.1003	(0.1169, 0.1203, 0.1256, 0.1275)
			V_6	0.0528	(0.0902, 0.0929, 0.0947, 0.0951)
			V_7	0.0369	(0.0705, 0.0731, 0.0734, 0.0746)
			V_8	0.0346	(0.0659, 0.0689, 0.0698, 0.0708)
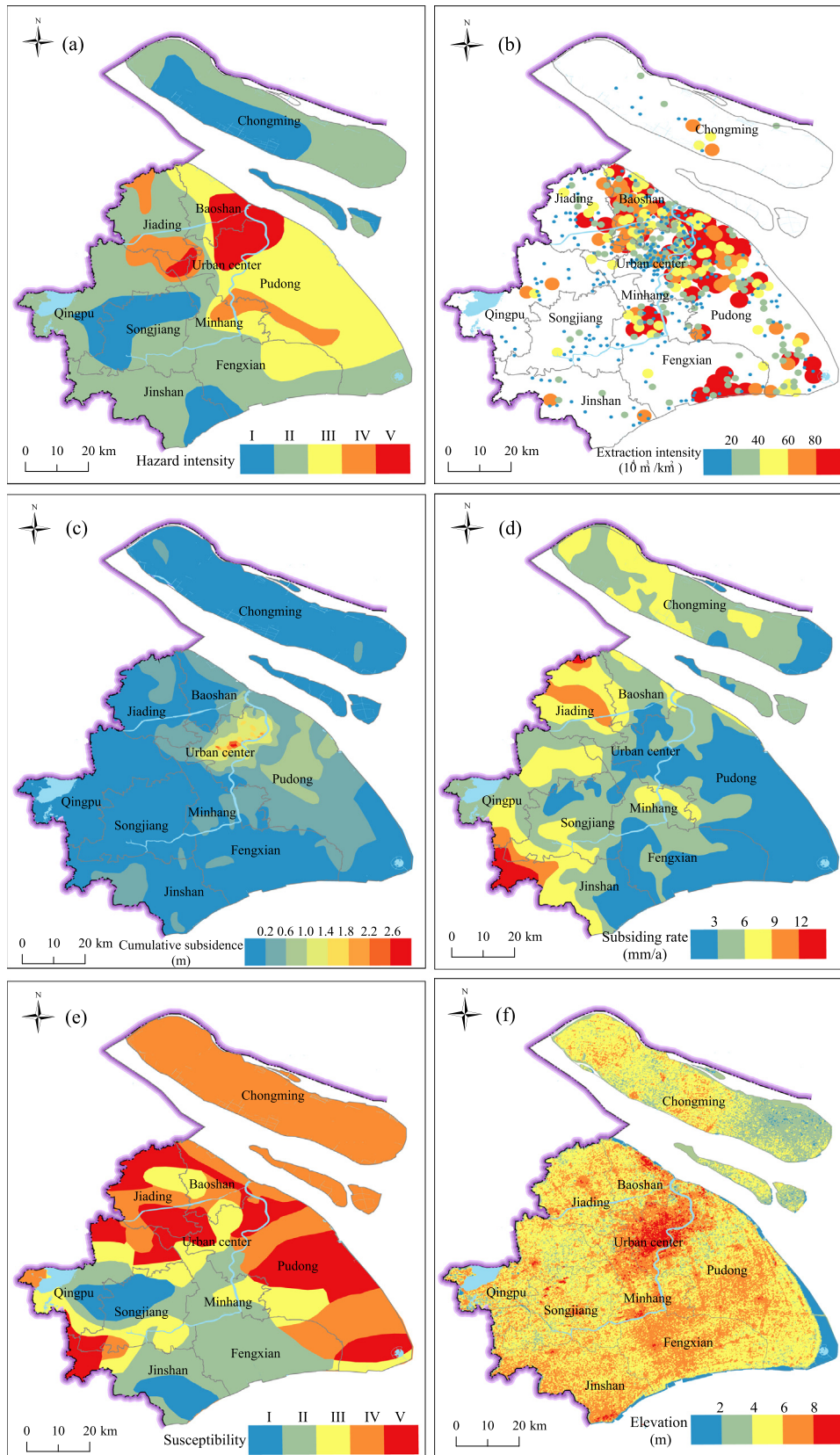
Fig. 4. Hazard index: (a) hazard intensity of land subsidence; (b) groundwater extraction intensity; (c) cumulative subsidence from 1921 to 2010; (d) subsiding rate; (e) potential land subsidence; (f) average ground elevation.
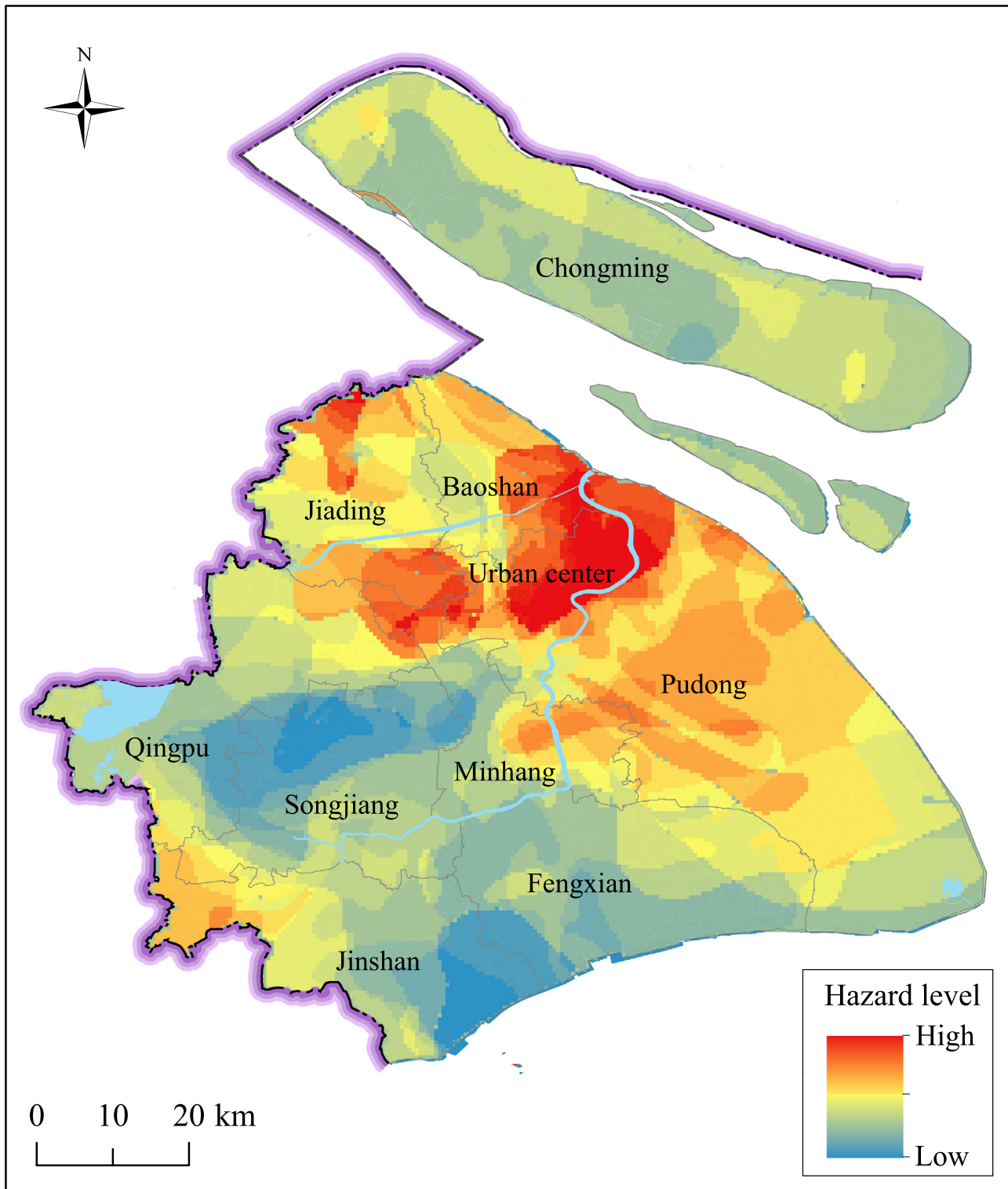
Fig. 5. Risk level of hazard index.

age path of groundwater, which results in the temporal–spatial redistribution of the groundwater level and land subsidence (Xu et al., 2012). This redistribution can cause a weight change in factors V_3 and V_4. Based on the identified factors, the hazard index and vulnerability index in risk assessment can be confirmed and the assessment structure can be established subsequently (see Fig. 3).

4.2.2. Judgement matrix with new questionnaire

As part of the consultation, the authors distributed 21 questionnaires to several experts including academics, contractors, client managers, and consultant engineers. The authors then selected the judgements of six experienced experts. These experts comprised three academics and three construction managers with more than 10-year experience. A summary of the questionnaire
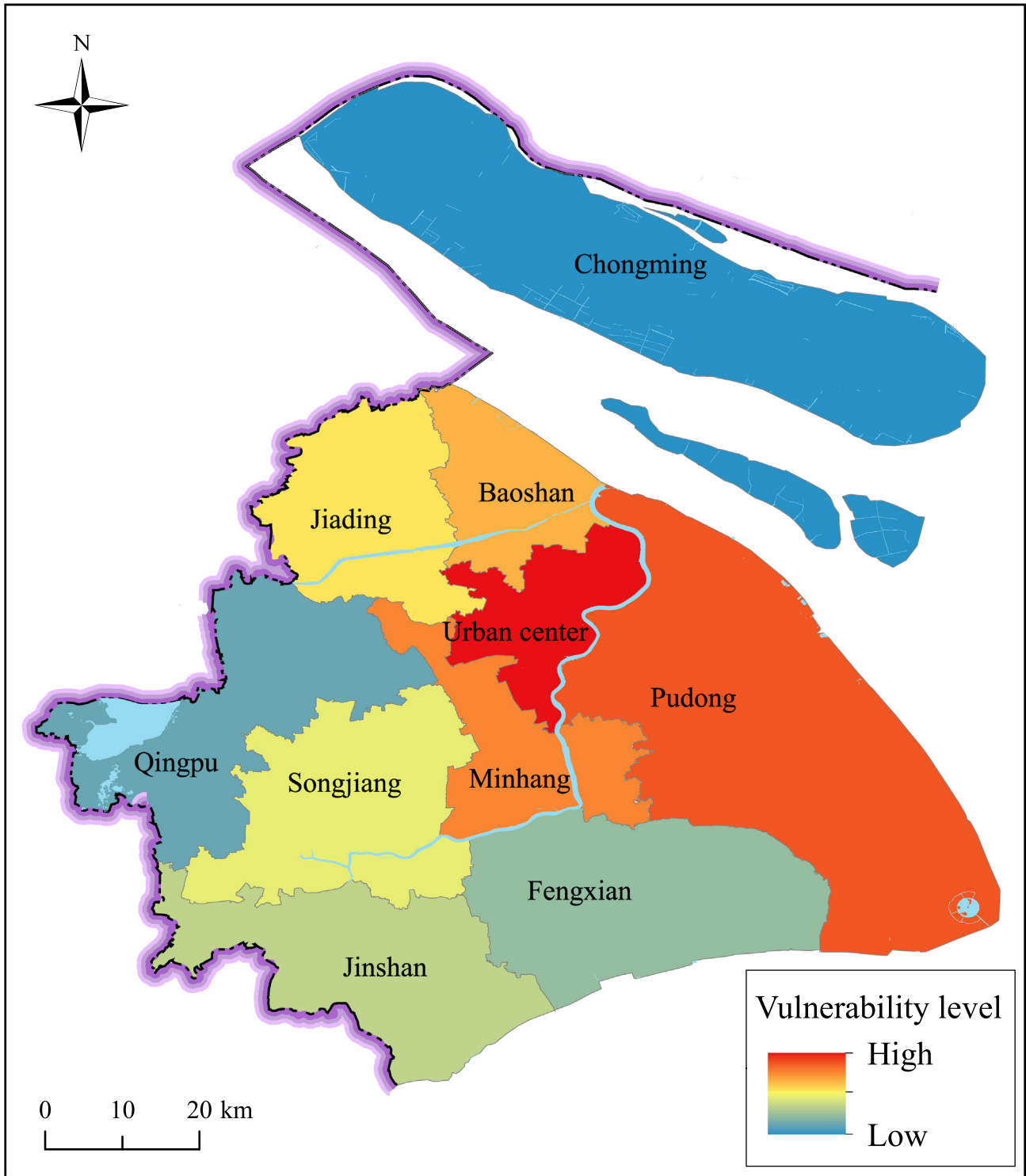
Fig. 6. Risk level of vulnerability index.

responses obtained from the six experts was presented in the data article (Lyu et al., 2019e).

Based on the statistical responses from the six experts, the authors established the judgement matrix by satisfying the consistency requirement. To elucidate how the judgement matrix is established, the expert responses of factors H_1 to H_6 in the hazard index are used as examples. The score for H_1 ranges from 7 to 9; therefore, H_1 is initially assigned a value of 7–9. It should be noted

that 9 is assigned four times. Similarly, $H_2 = 7$–9, while considering that both 7 and 9 are selected twice; $H_3 = 4$–7, with 4 assigned twice and 6 thrice; $H_4 = 4$–6, with 5 assigned thrice and 6 twice; $H_5 = 3$–5, with 4 assigned thrice and 5 twice; $H_6 = 1$–3, with 2 assigned thrice and 1 twice. Each element in the judgement matrix can be expressed as a ratio of one interval number to another, such as $\frac{H_1}{H_2} = \frac{7-9}{7-9}$, $\frac{H_1}{H_3} = \frac{7-9}{4-7}$, $\frac{H_1}{H_4} = \frac{7-9}{4-6}$, $\frac{H_1}{H_5} = \frac{7-9}{3-5}$, $\frac{H_1}{H_6} = \frac{7-9}{1-3}$, etc. Thus, a pairwise comparison judgement matrix can be obtained as follows.

$$\begin{bmatrix} 1 & \frac{7-9}{7-9} & \frac{7-9}{4-7} & \frac{7-9}{4-6} & \frac{7-9}{3-5} & \frac{7-9}{1-3} \\ \frac{7-9}{7-9} & 1 & \frac{7-9}{4-7} & \frac{7-9}{4-6} & \frac{7-9}{3-5} & \frac{7-9}{1-3} \\ \frac{4-7}{7-9} & \frac{4-7}{7-9} & 1 & \frac{4-7}{4-6} & \frac{4-7}{3-5} & \frac{4-7}{1-3} \\ \frac{4-6}{7-9} & \frac{4-6}{7-9} & \frac{4-6}{4-7} & 1 & \frac{4-6}{3-5} & \frac{4-6}{1-3} \\ \frac{3-5}{7-9} & \frac{3-5}{7-9} & \frac{3-5}{4-7} & \frac{3-5}{4-6} & 1 & \frac{3-5}{1-3} \\ \frac{1-3}{7-9} & \frac{1-3}{7-9} & \frac{1-3}{4-7} & \frac{1-3}{4-6} & \frac{1-3}{3-5} & 1 \end{bmatrix} \Rightarrow \begin{bmatrix} 1' & 1' & 2' & 3' & 2' & 2' \\ 1' & 1' & 2' & 2' & 2' & 2' \\ (\frac{1}{2})' & (\frac{1}{2})' & 1' & 3' & 3' & 2' \\ (\frac{1}{3})' & (\frac{1}{2})' & (\frac{1}{3})' & 1' & 5' & 6' \\ (\frac{1}{2})' & (\frac{1}{2})' & (\frac{1}{3})' & (\frac{1}{5})' & 1' & 3' \\ (\frac{1}{2})' & (\frac{1}{2})' & (\frac{1}{2})' & (\frac{1}{6})' & (\frac{1}{3})' & 1' \end{bmatrix}$$

This ratio can be considered to be a fuzzy number. By using trapezoidal fuzzy numbers to replace the ratio elements in the judgement matrix, a triangular fuzzy judgement matrix can be obtained. In the process of replacing each factor, it should be noted that the time required for assigning each score was taken into consideration for constructing the triangular fuzzy number to obtain a trapezoidal fuzzy number that is as close as possible to the original
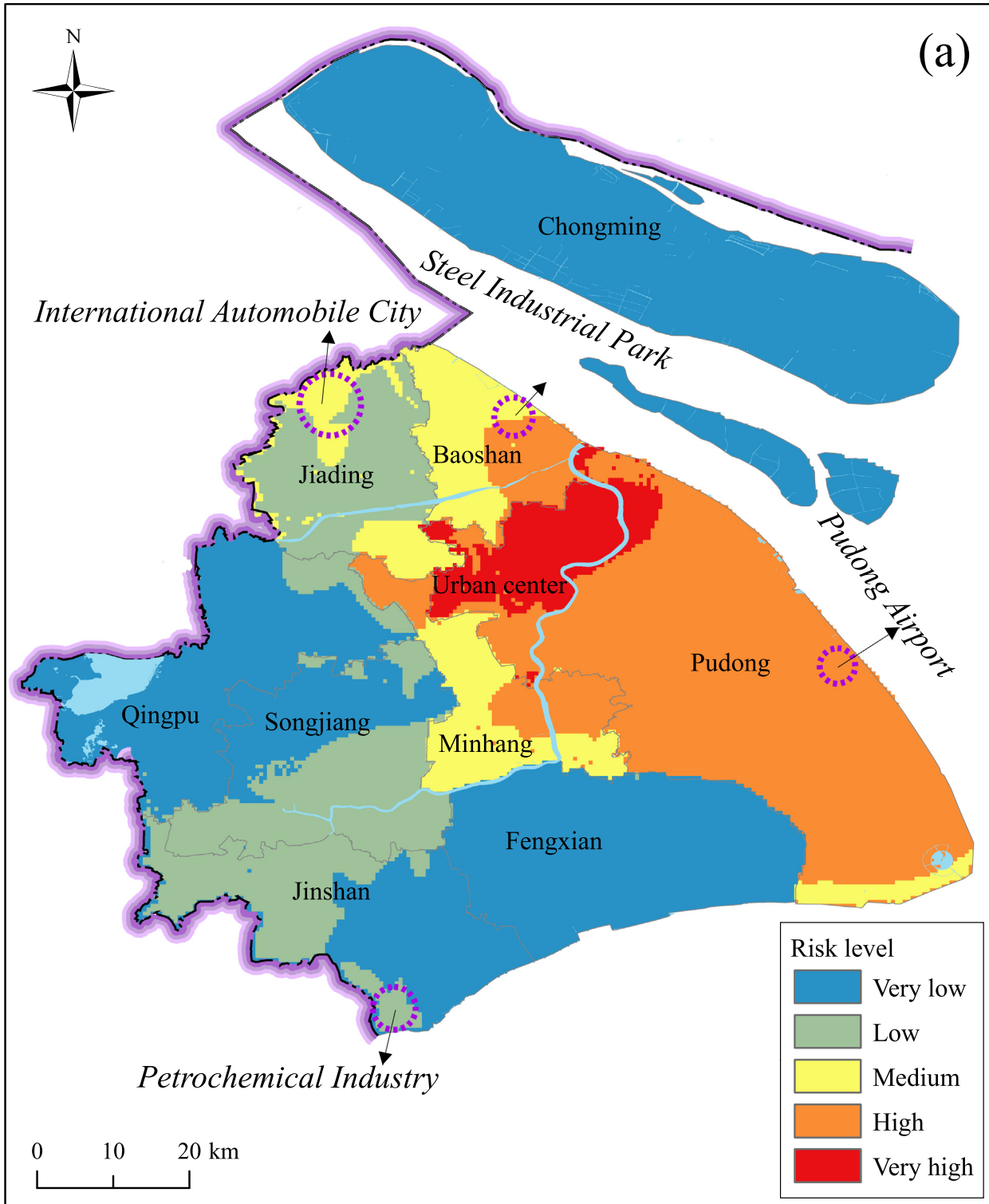

Fig. 7. Assessment results of the trapezoidal FAHP: (a) lower bound w_1, (b) left-medium w_2; (c) right-medium w_3; (d) upper bound w_4.
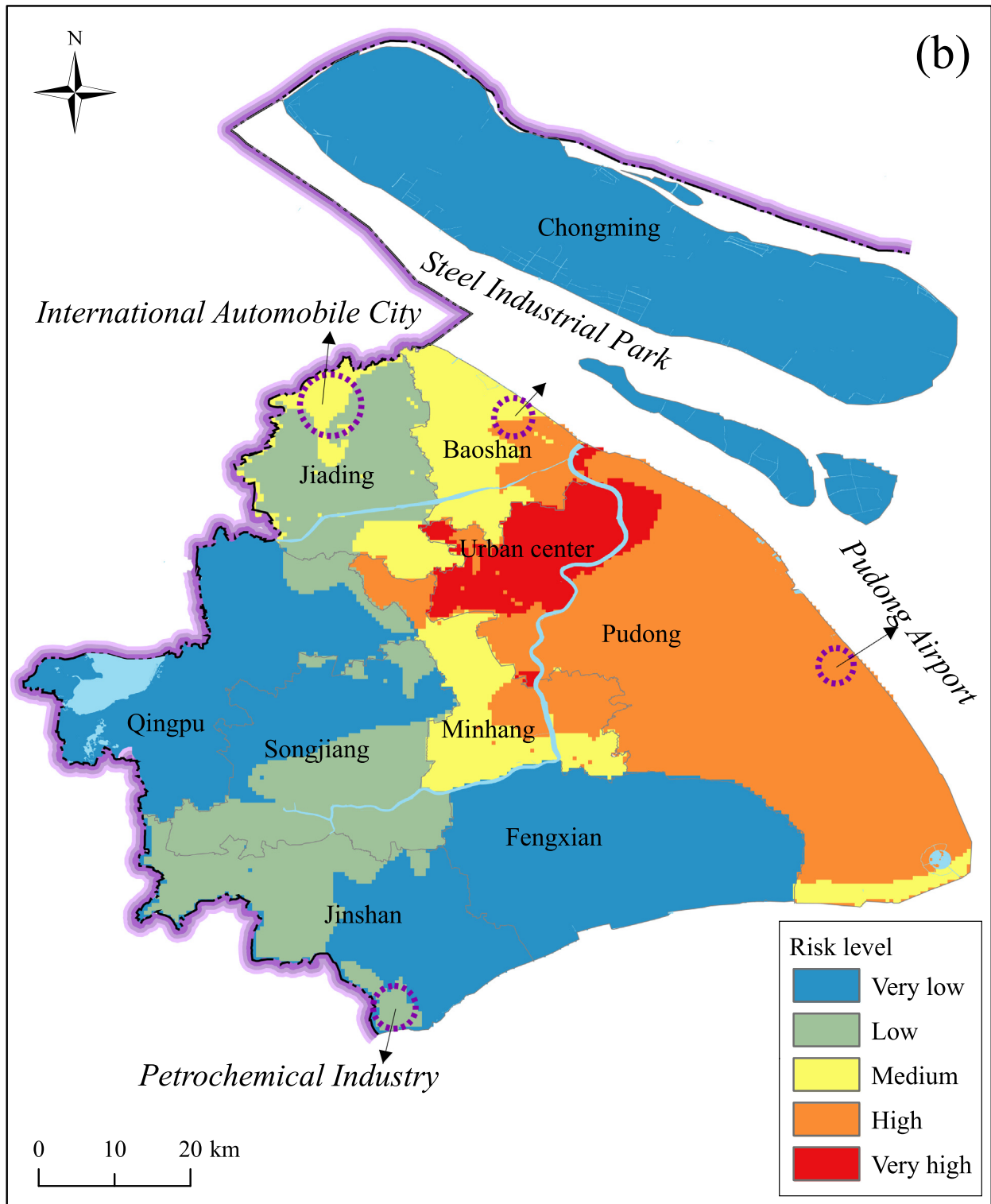
Fig. 7 (continued)

ratio. Finally, a concise judgement matrix P_{hazard} with an ordinary number can be determined. This matrix consists of trapezoidal fuzzy numbers with a CR of 0.0008, which indicates that the judgement matrix satisfies the consistency requirement ($CR < 0.1$). Similarly, the concise judgement matrix $P_{vulnerability}$ for the vulnerability index can also be obtained.

The extended trapezoidal judgement matrix can be calculated based on the concise judgement matrices P_{hazard} and $P_{vulnerability}$

and the linguistic variables with the corresponding trapezoidal fuzzy number. Tables B1 and B2 in Appendix B list the judgement matrices with trapezoidal fuzzy numbers. The fuzzy weight of the trapezoidal FAHP judgement matrix can be determined using Eqs. (8) to (11). In addition, the AHP weight (w) can also be obtained according to the concise judgement matrix. Table 2 lists the weights of the assessment factors determined using the trapezoidal FAHP and AHP methods.
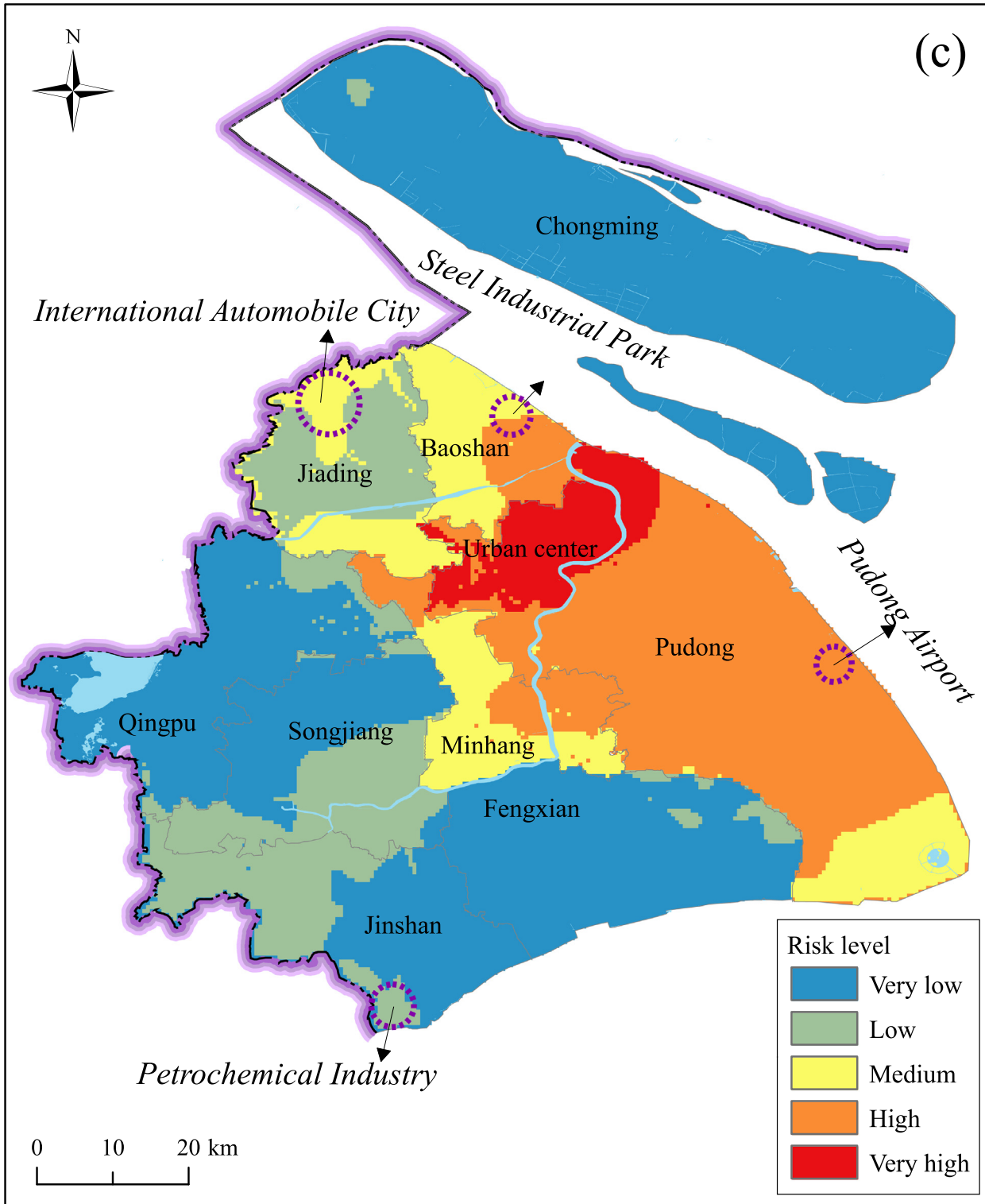
Fig. 7 (*continued*)

4.3. Results and analysis

4.3.1. Hazard index

Fig. 4 shows the map of six hazard index factors for Shanghai based on the collected data of the hazard index associated with land subsidence. These six factors include the historical hazard intensity of the land subsidence (Fig. 4a), groundwater extraction intensity (Fig. 4b), cumulative subsidence from 1921 to 2010

(Fig. 4c), historical subsiding rate (Fig. 4d), potential land subsidence (Fig. 4e), and average ground elevation (Fig. 4f). To facilitate the comparison between various factors, the value of each factor is normalised over the range from zero to one before conducting an overlay analysis.

According to the normalised factors with their corresponding weights listed in Table 1, the risk level of the hazard index (see Fig. 5) can be mapped using an overlay analysis in GIS. As shown
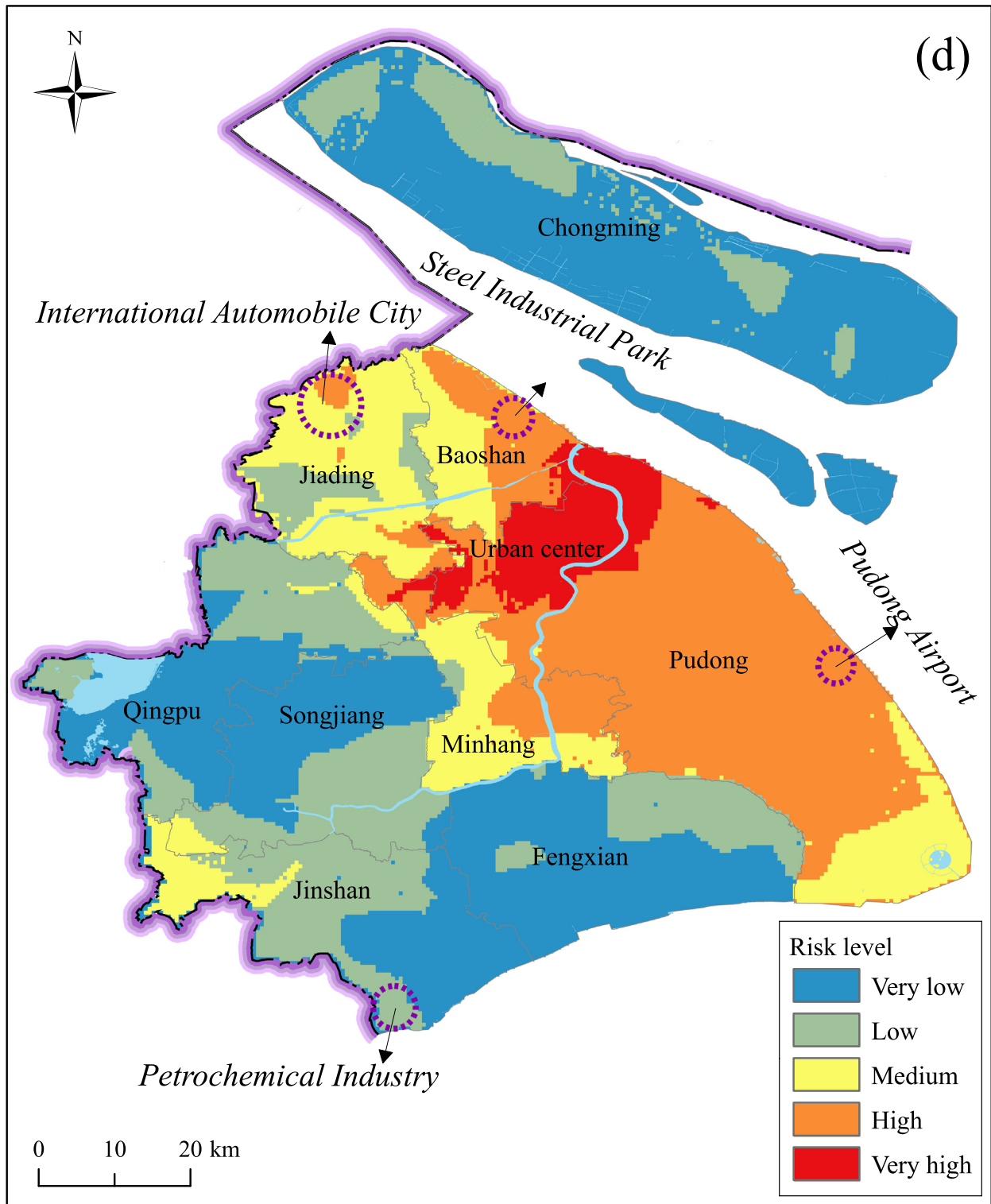
Fig. 7 (*continued*)

in Fig. 5, the hazard level of land subsidence in the urban centre and the adjacent Baoshan district are higher than those in other regions on the comprehensive combination of these six factors. The result of the hazard index is similar to that of the historical hazard intensity of land subsidence (Fig. 4a) because the weight of this factor is the largest. During the overlay analysis, the factor with the largest weight is critical to the assessment result. The visualisation of the hazard level was mapped using a raster calculator in GIS.

4.3.2. Vulnerability index

The vulnerability factors related to the land subsidence of 11 districts in Shanghai (Wang et al. 2014; SSY, 2017) were presented in a data article (Lyu et al., 2019e). Based on the viewpoints from the six experts, the factors of V_1, V_2, V_3, V_4, V_5, and V_6 are positive factors, whereas V_7 and V_8 are negative factors. The normalised factors can be obtained using Eqs. (3) and (4). Subsequent to the normalisation, the spatial distribution of the normalised factors for district division can be visualised using GIS. The normalised fac-
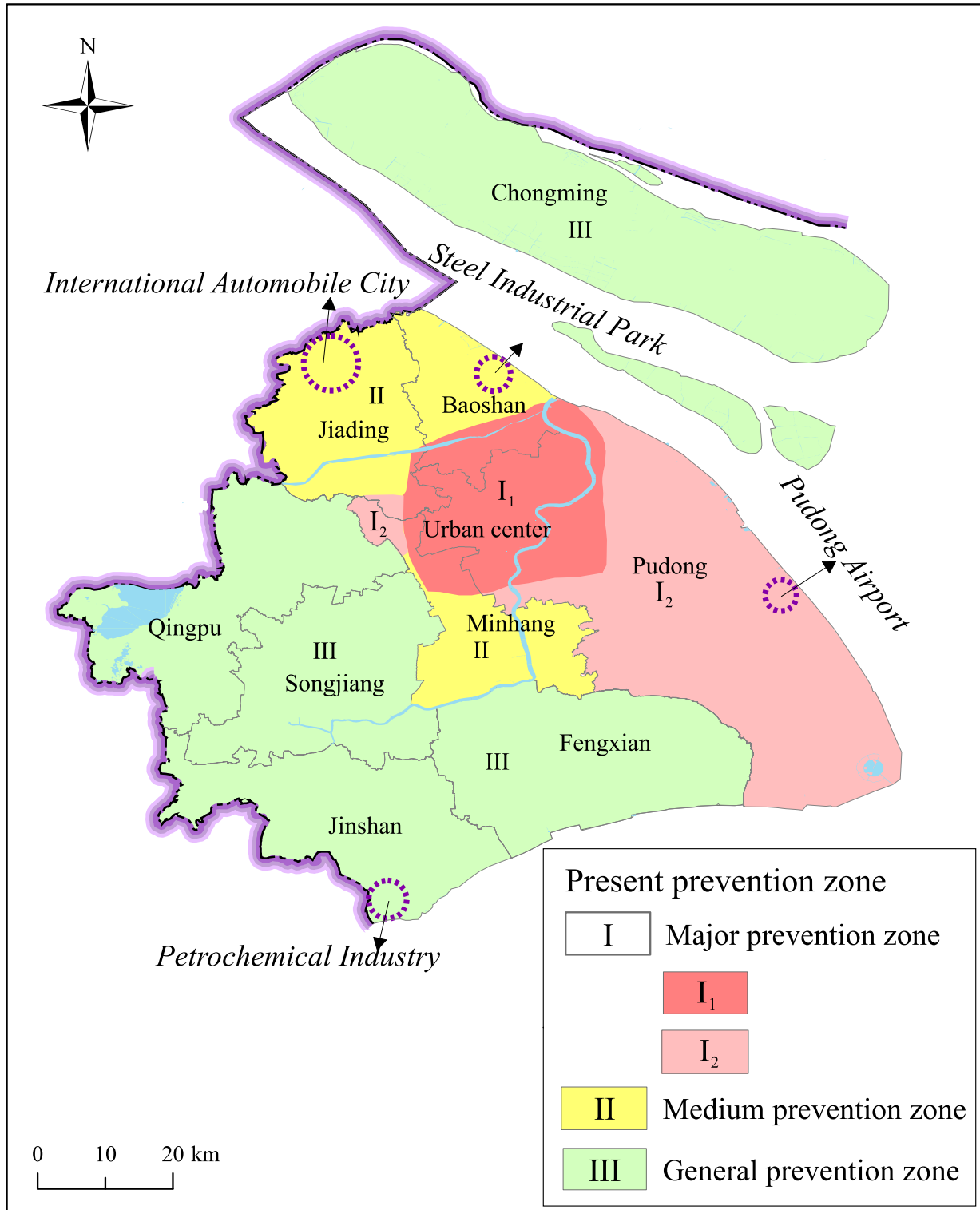
Fig. 8. Present prevention zone for land subsidence in Shanghai (modified from Wang et al., 2014).

tors combined with their corresponding weights can yield the spatial distribution of the risk level of the vulnerability index. Fig. 6 shows the spatial distribution of the risk level of the vulnerability index. As shown in Fig. 6, the urban centre has the highest risk level of vulnerability followed by the Pudong district. Furthermore, the Chongming district has the lowest risk level of vulnerability.

4.3.3. Risk level of land subsidence

Subsequent to obtaining the assessment results of the risk level of the hazard index (see Fig. 5) and vulnerability index (see Fig. 6), the risk level with a fuzzy weight can be evaluated. Fig. 7 shows the assessment result of the trapezoidal FAHP with fuzzy weights w_1, w_2, w_3, and w_4. As shown in Fig. 7, for all four results with a lower bound w_1 (Fig. 7a), left-medium w_2 (Fig. 7b), right-medium
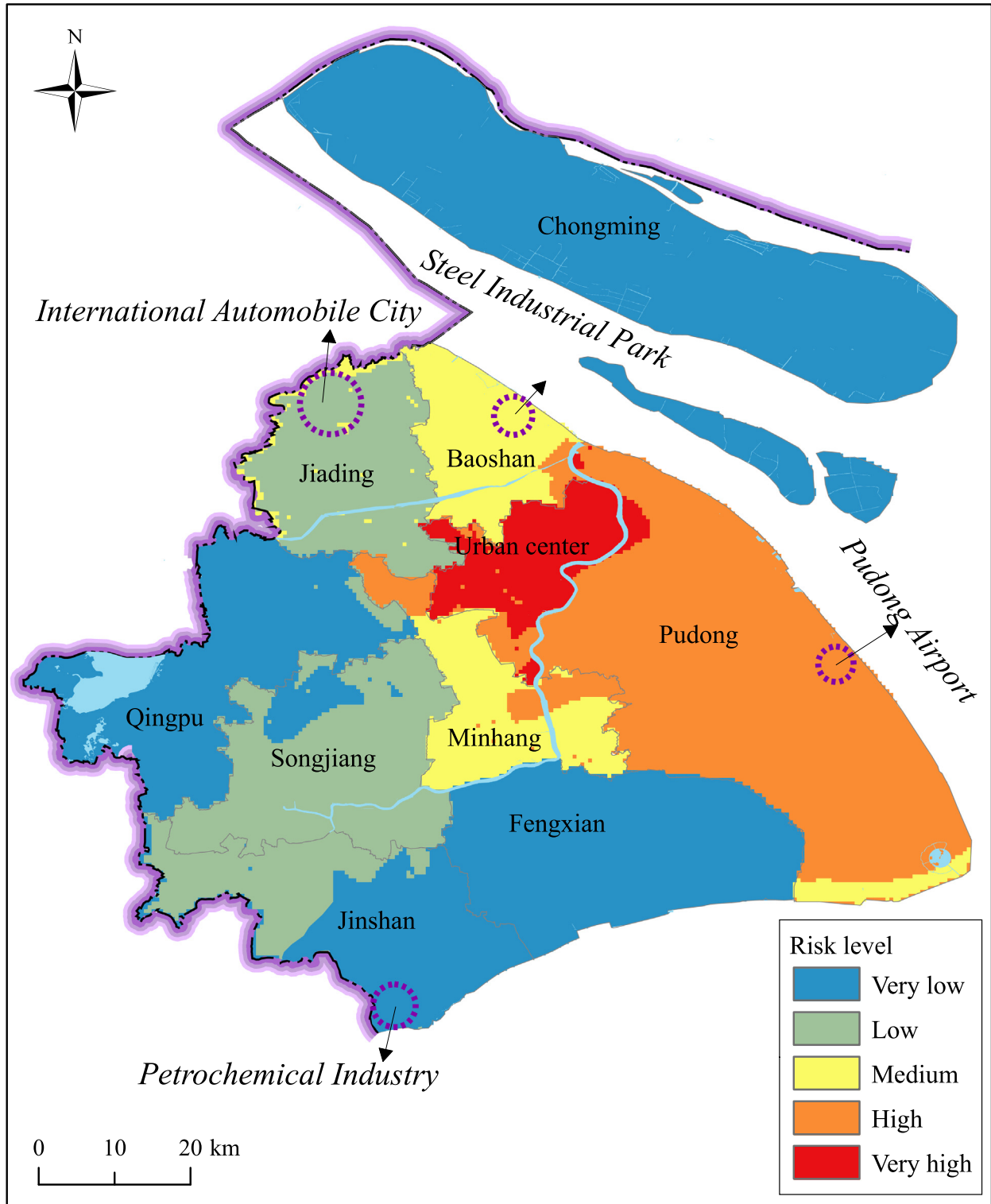
Fig. 9. Assessment result of AHP method.

w_3 (Fig. 7c), and upper bound w_4, the evaluated risk level of the urban centre was very high. The evaluated risk level of the region adjacent to the urban centre and Pudong district was high. The medium-risk-level area was located in some regions of the Baoshan, Jiading, and Minhang districts. The Qingpu, Fengxian, and Chongming districts were assessed with low-risk levels, as

their hazard and vulnerability levels were low (see Figs. 5 and 6). As shown in Fig. 7, the proposed method can be used to assess the vulnerable risk of regions with significant facilities accurately, such as the Steel Industrial Park in Baoshan district, Anting Shanghai International Automobile City in Jiading, Petrochemical Industrial in Jinshan, and Pudong International Airport. In addition, the

location of the International Automobile City was assessed at a high-risk level as shown in Fig. 7d, whereas the others were assessed at the medium risk level. This is owing to the greatest weight of the upper bound w_4 in the trapezoidal FAHP. During the overlay analysis in GIS, the factor with a larger weight has a more critical effect on the assessment result.

4.4. Validation and discussion

4.4.1. Validation

The current code for land subsidence management was based on a series investigation conducted by the Shanghai Geological Investigation Institute (Shen and Xu, 2011; Wang et al. 2014; Xu et al., 2016; SGII, 2016). Fig. 8 shows the current prevention zone division for land subsidence that has been used by the Shanghai government. By comparing the results presented in Figs. 7 and 8, it was observed that the assessed area with a high risk in Fig. 7 was located in the major prevention zone (I) in Fig. 8. The area with a medium risk in Fig. 7 corresponds to the medium prevention zone (II) in Fig. 8. Moreover, the area with a low risk in Fig. 7 corresponds to the general prevention zone (III) in Fig. 8. Therefore, it can be concluded that the assessment result obtained using the proposed method is reasonable as compared with the current code based on a large quantity of geological investigation.

It should be noted that the current prevention zone executed by the Shanghai government presents some limitations, which has resulted in the significant industrial facilities not being protected effectively. For example, the protection level is low for some significant industry facilities and infrastructure, such as Steel Industrial Park in Baoshan district, Anting Shanghai International Automobile City in Jiading district, and Petrochemical Industrial in Jinshan district. Moreover, the assessment result obtained using the trapezoidal FAHP presents a high-risk level for these significant infrastructures. The Steel Industrial Park and Anting Shanghai International Automobile City play significant roles in industrial production. Petrochemical Industrial mainly produces chemical products, which is vulnerable to land subsidence. These infrastructures will be significantly affected by land subsidence. Therefore, more attention should be focused on the zones with significant infrastructures to protect them from land subsidence.

4.4.2. Comparison between the results from trapezoidal FAHP and AHP

Fig. 9 shows the assessment result obtained using the AHP method. The result was evaluated using the traditional AHP weight. As shown in Fig. 9, Petrochemical Industrial in Jinshan was assessed at a very low risk level by the AHP, whereas the trapezoidal FAHP assessed it at a low risk level. The International Automobile City in Jiading was assessed at a low risk level by the AHP, but it was found to be at the medium-risk (MR) and high-risk levels by the trapezoidal FAHP. The Steel Industrial Park in Baoshan district was assessed at the medium risk by the AHP, but it was assessed at the high-risk level by the trapezoidal FAHP. The risk levels of these regions with significant infrastructures as obtained from trapezoidal FAHP are higher than those obtained using the original AHP. The comparison reveals that the trapezoidal FAHP can capture the high risks for significant infrastructures, which can thus provide a better risk assessment for urban infrastructures.

To identify the differences between the trapezoidal FAHP and AHP results, the area with different risks can be accounted using GIS. Fig. 10 shows the region with different risk levels obtained by the trapezoidal FAHP and AHP. As shown in Fig. 10, the area with the high- and very-high-risk levels obtained from the trapezoidal FAHP is larger than that obtained from the AHP. Fig. 11 pre-
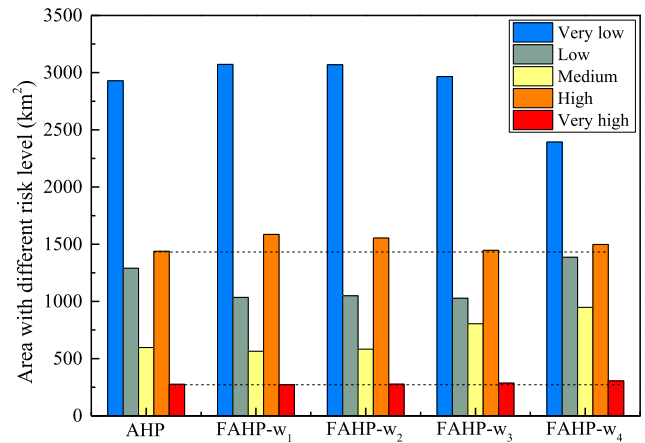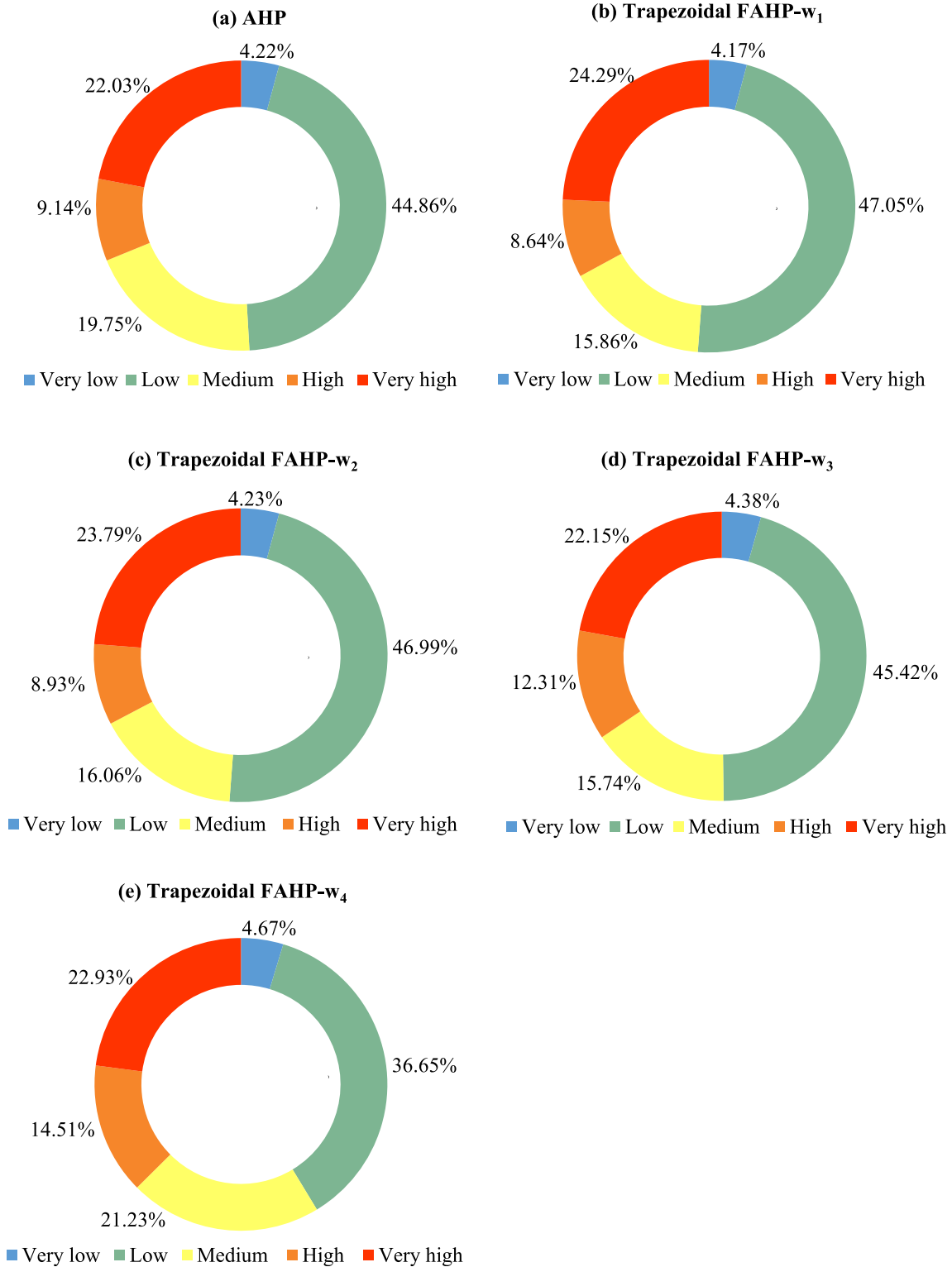

Fig. 10. Comparison of the area with different risk levels between trapezoidal FAHP and AHP.

sents the percentage of different risk levels as obtained using the AHP and trapezoidal FAHP. The percentage is calculated using the (area with one risk level/the total region) × 100%. The area with one risk level can be extracted from GIS. The percentage of very high risk level obtained using the AHP weight is 22.0%, which is less than that obtained on using the weight of the lower bound (24.3%), left-medium (23.8%), right-medium (22.2%), and upper bound (22.9%) of the trapezoidal FAHP. Therefore, the trapezoidal FAHP yields a broader assessment result of high-risk regions than the AHP. As the trapezoidal FAHP comprises the use of trapezoidal fuzzy numbers, which have four weights (lower, left-medium, right-medium, and upper bounds), each weight can provide an assessed result. Thus, the trapezoidal FAHP can yield an assessment range with four choices for decision-making. However, the AHP yields only one assessment result, which may demonstrate biases.

5. Conclusions

This study applied the trapezoidal FAHP with a new questionnaire for assessing the risk induced by land subsidence for urban infrastructures in mega-cities. A case study of land subsidence in Shanghai was presented to illustrate the application of the new questionnaire in the trapezoidal FAHP to assess the risks. The assessment results were validated by the present prevention zone for land subsidence in Shanghai. The major findings are summarised as follows:

(1) A trapezoidal fuzzy number can become a triangular/interval fuzzy or a crisp number, which can arithmetically handle and intuitively interpret fuzzy numbers in a variable manner. The application of trapezoidal fuzzy numbers in the FAHP is an efficient method for assessing the infrastructure risk induced by land subsidence.

(2) The trapezoidal FAHP comprised the use of trapezoidal fuzzy numbers for expressing the relative importance between the assessment factors; it could tolerate the uncertainties of one factor to another. The trapezoidal FAHP could yield a more reasonable assessment than the AHP in that the trapezoidal FAHP could reflect the actual situation during decision-making.

(3) In the case study, the risk induced by land subsidence was assessed with the consideration of blocking effects from underground structures, which caused the temporal–spatial

Fig. 11. Percentage of different risk level from AHP and trapezoidal FAHP: (a) AHP; (b) lower bound w_1, (c) left-medium w_2; (d) right-medium w_3; (e) upper bound w_4.

redistribution of groundwater level and land subsidence. The results were validated using the current prevention zone division for land subsidence.

(4) The risk of the locations with significant infrastructures assessed using the trapezoidal FAHP is higher than that using the AHP. The percentage of high-risk levels obtained using the trapezoidal FAHP is greater than that using the AHP. The comparison indicates that the trapezoidal AHP with the new questionnaire can provide a more reasonable assessment result.

Declaration of Competing Interest

Acknowledgements

Appendix A. Supplementary data

Supplementary data to this article can be found online at https://doi.org/10.1016/j.scitotenv.2019.135310.

References

Chai, J.C., Shen, S.L., Zhu, H.H., Zhang, X.L., 2004. Land subsidence due to groundwater drawdown in Shanghai. Geotechnique, ICE, UK 54 (2), 143–147.

DGJ08-37-2012. 2012. Code for investigation of geotechnical engineering in Shanghai. Shanghai Urban Construction and Communications Commission, Shanghai. (in Chinese).

Godschalk, D.R., 2003. Urban hazard migration: creating resilient cities. Nat. Hazard. Rev. 4 (3), 136–143.

Ishikawa, A., Amagasa, M., Shiga, T., Tomizawa, G., Tatsuta, R., Mieno, H., 1993. The max-min Delphi method and fuzzy Delphi method via fuzzy integration. Fuzzy Sets Syst. 55 (3), 241–253.

Jin, Y.F., Yin, Z.Y., Shen, S.L., Hicher, P.Y., 2016. Selection of sand models and identification of parameters using an enhanced genetic algorithm. Int. J. Numer. Anal. Meth. Geomech. 40, 1219–1240.

Jin, Y.F., Yin, Z.Y., Wu, Z.X., Zhou, W.H., 2018. Identifying parameters of easily crushable sand and application to offshore pile driving. Ocean Eng. 154, 416–429.

Jin, Y.F., Yin, Z.Y., Zhou, W.H., Huang, H.W., 2019a. Multi-objective optimization-based updating of predictions during excavation. Eng. Appl. Artif. Intell. 78, 102–123.

Jin, Y.F., Yin, Z.Y., Zhou, W.H., Yin, J.H., Shao, J.F., 2019b. A single-objective EPR based model for creep index of soft clays considering L_2 regularization. Eng. Geol. 248 (8), 242–255.

Kamal, H.A., Ayyub, B.M., Abdullah, W.A., 2013. Land subsidence in arid terrain: methodology toward risk analysis. Nat. Hazard. Rev. 14 (4), 268–280.

Laarhoven, P.J.M.V., Pedrycz, W., 1983. A fuzzy extension of saaty's priority theory. Fuzzy Sets Syst. 11 (1–3), 199–227.

Lee, S., Park, I., 2013. Application of decision tree model for the ground subsidence hazard mapping near abandoned underground coal mines. J. Environ. Manage. 127, 166–176.

Li, F., Phoon, K.K., Du, X., Zhang, M., 2013. Improved AHP method and its application in risk identification. J. Constr. Eng. Manage. 139 (3), 312–320. https://doi.org/10.1061/(ASCE)CO.1943-7862.0000605.

Lyu, H.M., Sun, W.J., Shen, S.L., Arulrajah, A., 2018. Flood risk assessment in metro systems of mega-cities using a GIS-based modeling approach. Sci. Total Environ. 626, 1012–1025. https://doi.org/10.1016/j.scitotenv.2018.01.138.

Lyu, H.-M., Shen, S.-L., Yang, J., Yin, Z.-Y., 2019a. Inundation analysis of metro systems with the storm water management model incorporated into a geographical information system: a case study in Shanghai.. Hydrology and Earth System Sciences 23 (10), 4293–4307. https://doi.org/10.5194/hess-23-4293-2019.

Lyu, H.M., Shen, S.L., Zhou, A.N., Yang, J., 2019b. Perspectives for flood risk assessment and management for mega-city metro system. Tunn. Undergr. Sp. Technol. 84 (2019), 31–44. https://doi.org/10.1016/j.tust.2018.10.019.

Lyu, H.M., Shen, S.L., Zhou, A.N., Zhou, W.H., 2019c. Flood risk assessment of metro systems in a subsiding environment using the interval FAHP-FCA approach. Sustainable Cities Soc. 50, (2019). https://doi.org/10.1016/j.scs.2019.101682 101682.

Lyu, H.M., Sun, W.J., Shen, S.L., Zhou, A.N., 2019d. Risk assessment using a new consulting process in fuzzy AHP. J. Constr. Eng. Manage. https://doi.org/10.1061/(ASCE)CO.1943-7862.0001757.

Lyu, H.-M., Shen, S.-L., Zhou, A., Yang, J., 2019e. Data in Risk assessment of mega-city infrastructures related to land subsidence using improved trapezoidal FAHP. Data in Brief. Under Review.

Ma, L., Xu, Y.S., Shen, S.L., Sun, W.J., 2014. Evaluation of the hydraulic conductivity of aquifers with piles. Hydrogeol. J. 22 (2), 371–382.

Peng, J., Peng, F.L., 2018. A GIS-Based evaluation method of underground space resource for urban spatial planning: Part 1 Methodology. Tunn. Undergr. Space Technol. 74, 82–95.

Prascevic, N., Prascevic, Z., 2017. Application of Fuzzy AHP for ranking and selection of alternatives in construction project management. J. Civil Eng. Manage. 23 (8), 1123–1135.

Qiao, Y.K., Peng, F.L., Wang, Y., 2017. Monetary valuation of urban underground space: A critical issue for the decision-making of urban underground space development. Land Use Policy. 69 (12), 12–24.

Saaty, T.L., 1996. Decision making with dependence and feedback: the analytic network process. RWS Publication, Pittsburgh.

Saaty, T.L., 2004. Decision making—the analytic hierarchy and network processes (AHP/ANP). J. Syst. Sci. Syst. Eng. 13 (1), 1–35.

Sadiq, R., Tesfamariam, S., 2009. Environmental decision-making under uncertainty using intuitionistic fuzzy analytic hierarchy process (IF-AHP). Stoch. Env. Res. Risk Assess. 23 (1), 75–91.

SGII, 2016. Shanghai Geological Investigation Institute, The report of key technology on zoning control for land subsidence management. (in Chinese)

SSY Shanghai Statistical Yearbook available online: http://www.stats-sh.gov.cn/ 2017 accessed on 8 March, 2018

Shen, S.L., Xu, Y.S., 2011. Numerical evaluation of land subsidence induced by groundwater pumping in Shanghai. Can. Geotech. J. 48 (9), 1378–1392.

Shen, S.L., Ma, L., Xu, Y.S., Yin, Z.Y., 2013. Interpretation of increased deformation rate in aquifer IV due to groundwater pumping in Shanghai. Can. Geotech. J. 50, 1129–1142.

Shen, S.L., Wu, H.N., Cui, Y.J., Yin, Z.Y., 2014. Long-term settlement behavior of the metro tunnel in Shanghai. Tunn. Undergr. Space Technol. 40, 309–323.

Shen, S.L., Wu, Y.X., Misra, A., 2017. Calculation of head difference at two sides of a cut-off barrier during excavation dewatering. Comput. Geotech. 91, 192–202. https://doi.org/10.1016/j.compgeo.2017.07.014.

Sierra, L.A., Yepes, V., Pellicer, E., 2018. A review of multi-criteria assessment of the social sustainability of infrastructures. J. Cleaner Prod. 187, 496–513.

Wang, H.M., Wang, Y., Jiao, X., Qian, G.R., 2014. Risk management of land subsidence in Shanghai. Desalin. Water Treat. 52 (4–6), 1122–1129.

Wang, X.W., Yang, T.L., Xu, Y.S., Shen, S.L., 2019. Evaluation of optimized depth of waterproof curtain to mitigate negative impacts during dewatering. J. Hydrol. 577, (2019). https://doi.org/10.1016/j.jhydrol.2019.123969 123969.

Wu, Y.X., Shen, S.L., Yuan, D.J., 2016. Characteristics of dewatering induced drawdown curve under blocking effect of retaining wall in aquifer. J. Hydrol. 539, 554–566.

Wu, Y.X., Lyu, H.M., Han, J., Shen, S.L., 2019. Dewatering–induced building settlement around a deep excavation in soft deposit in Tianjin, China. J. Geotech. Geoenviron. Eng. ASCE 145 (5), 05019003. https://doi.org/10.1061/(ASCE)GT.1943-5606.0002045.

Wu, Y.X., Shen, J.S., Cheng, W.C., Hino, T., 2017a. Semi-analytical solution to pumping test data with barrier, wellbore storage, and partial penetration effects. Engineering Geology 226 (2017), 44–51. https://doi.org/10.1016/j.enggeo.2017.05.011.

Wu, H.N., Shen, S.L., Yang, J., 2017b. Identification of tunnel settlement caused by land subsidence in soft deposit of Shanghai. J. Perform. Constr. Facil 31 (6), 4017092.

Xu, Y.S., Ma, L., Shen, S.L., Sun, W.J., 2012. Evaluation of land subsidence by considering underground structures penetrated into aquifers in Shanghai. Hydrogeol. J. 20 (8), 1623–1634.

Xu, Y.S., Shen, S.L., Du, Y.J., Chai, J.C., Horpibulsuk, S., 2013. Modelling the cutoff behavior of underground structure in multi-aquifer-aquitard groundwater system. Nat. Hazards 66 (2), 731–748. https://doi.org/10.1007/s11069-012-0512-y.

Xu, Y.S., Shen, S.L., Ren, D.J., Wu, H.N., 2016. Factor analysis of land subsidence in Shanghai: a view based on Strategic Environmental Assessment. Sustainability 8 (2016), 573(1–12). doi:10.3390/su8060573

Xu, Y.S., Yan, X.X., Shen, S.L., Zhou, A.N., 2019. Experimental investigation on the blocking of groundwater seepage from a waterproof curtain during pumped dewatering in an excavation. Hydrogeol. J. 27 (7), 2659–2672. https://doi.org/10.1007/s10040-019-01992-3.

Yi, L.X., Jie, W., Shao, C.Q., Guo, J.W., Jiang, Y.X., Liu, B., 2010. Land subsidence disaster survey and its economic loss assessment in Tianjin, China. Nat. Hazards Rev. 11 (1), 35–41.

Yin, Z.Y., Karstunen, M., Chang, C.S., Koskinen, M., Lojander, M., 2011. Modeling time-dependent behavior of soft sensitive clay. J. Geotech. Geoenviron. Eng. 137 (11), 1103–1113.

Yin, Z.Y., Zhu, Q.Y., Yin, J.H., Ni, Q., 2014. Stress relaxation coefficient and formulation for soft soils. Géotech. Lett. 4 (1), 45–51.

Yin, Z.Y., Jin, Y.F., Shen, S.L., Huang, H.W., 2017. An efficient optimization method for identifying parameters of soft structured clay by an enhanced genetic algorithm and elastic–viscoplastic model. Acta Geotech. 12, 849. https://doi.org/10.1007/s11440-016-0486-0.

Yin, Z.Y., Jin, Y.F., Shen, J.S., Hicher, P.Y., 2018. Optimization techniques for identifying soil parameters in geotechnical engineering: comparative study and enhancement. Int. J. Numer. Anal. Meth. Geomech. 42, 70–94.

Zou, Q., Zhou, J., Zhou, C., Song, L., Guo, J., 2013. Comprehensive flood risk assessment based on set pair analysis-variable fuzzy sets model and fuzzy AHP. Stochastic Environ. Res. Risk Assess. 27 (2), 525–546.

Zhu, Q.Y., Yin, Z.Y., Hicher, P.Y., Shen, S.L., 2016. Nonlinearity of one-dimensional creep characteristics of soft clays. Acta Geotech. 11, 887. https://doi.org/10.1007/s11440-015-0411-y.